Composites Science and Technology 166 (2018) 150–159

Contents lists available at ScienceDirect

Composites Science and Technology

journal homepage: http://www.elsevier.com/locate/compscitech

Advanced carbon fiber composite out-of-autoclave laminate manufacture via nanostructured out-of-oven conductive curing

Jeonyoon Lee [a], Xinchen Ni [a], Frederick Daso [b], Xianghui Xiao [c], Dale King [d], Jose Sánchez Gómez [e], Tamara Blanco Varela [e], Seth S. Kessler [f], Brian L. Wardle [b, *]

[a] Department of Mechanical Engineering, Massachusetts Institute of Technology, Cambridge, MA 02139, USA
[b] Department of Aeronautics and Astronautics, Massachusetts Institute of Technology, Cambridge, MA 02139, USA
[c] Advanced Photon Source, Argonne National Laboratory, Lemont, IL 60439, USA
[d] Emerging Technologies & Concepts, Airbus Operations Ltd., Aerospace Avenue, Filton, Bristol BS34 7PA, UK
[e] Materials & Processes, Airbus Operations S.L., Paseo John Lennon, Getafe 28906, Spain
[f] Metis Design Corporation, 205 Portland Street, Boston, MA 02114, USA

ARTICLE INFO

Article history:
Received 1 September 2017
Received in revised form
8 February 2018
Accepted 19 February 2018
Available online 26 February 2018

Keywords:
Carbon nanotubes
Prepreg
Out-of-Autoclave
Conductive curing
Resistive heating

ABSTRACT

Next-generation composite manufacturing processes are needed to overcome several limitations of conventional manufacturing processes (e.g., high energy consumption). Here we explore, via experiments and modeling, the characteristics of the newly developed out-of-oven (OoO) curing technique that cures a composite laminate via resistive heating of a carbon nanotube film. When compared to oven curing of an aerospace-grade out-of-autoclave (OoA) carbon fiber prepreg advanced composite laminate, the OoO curing reduces energy consumption by over two orders of magnitude (14 vs. 0.1 MJ). Thermophysical and mechanical tests including differential scanning calorimetry (DSC), dynamic mechanical analysis (DMA), short beam shear (SBS), and *ex-situ* and *in-situ* double-edge notch tension (DENT) indicate that the physical and mechanical properties of OoO-cured laminates are equivalent to those of oven-cured (baseline) laminates. In addition to energy savings, the OoO curing process has the potential to reduce part-to-part variations through improved spatiotemporal temperature control.

1. Introduction

Manufacturing of aerospace structural composites has traditionally focused on using autoclaves to achieve high-quality reproducible parts, including high fiber volume fractions and low porosity [1,2]. Specifically, carbon fibers, which are pre-impregnated with a thermoset or thermoplastic resin to form prepreg sheets, are primarily used for autoclave processing techniques because of their ease of use and exceptional mechanical performance. However, manufacturing composites within an autoclave is accompanied by high acquisition and operation costs due to the necessity of a specialized heated pressure vessel to suppress the formation of voids. Furthermore, the capacity of autoclaves limits the size and design of parts, and the production rate is primarily affected by autoclave availability. As a result, there has been an increasing interest in the development of alternative techniques. For example, the previous studies reported manufacturing approaches changing the method of heating such as microwave heating, induction heating, laser heating, and resistive heating of carbon fibers or carbon nanotube (CNT) fillers in composites [3–6]. Additionally, specially-formulated and designed prepregs that can be cured in an oven (out-of-autoclave, or OoA prepregs) have been recently developed to remove the need of an autoclave [7,8].

OoA prepregs with oven curing have been introduced commercially as an alternative to autoclave-cured prepreg manufacturing. In contrast to the autoclave prepregs, OoA prepregs do not require the use of pressure vessels to achieve a void-free laminate because of their formulation and unique structure; dry regions between resin-rich regions in OoA prepregs function as built-in void extraction channels [8–15]. Thus, OoA prepregs can be cured with conventional thermal ovens thereby allowing lower cost manufacturing than using autoclave-cured prepregs [16,17]. Nonetheless, even the use of conventional ovens is not completely ideal from a manufacturing perspective. Heat transfer is still based on convection, which leads to inefficiencies and to spatial gradients

* Corresponding author.
E-mail address: wardle@mit.edu (B.L. Wardle).

https://doi.org/10.1016/j.compscitech.2018.02.031
0266-3538/

in cure and stress due to convective-to-conductive interactions between the oven gas medium (usually air) and the cure materials [18–20]. This also drives part-to-part variability, and fabrication is still limited because of its fixed geometry despite advantages of an oven vs. an autoclave.

Given the limitations above, the concept of an out-of-oven (OoO) process has been proposed, which uses a CNT film as a heating element directly integrated into the surface of a laminate so that curing does not require any heating vessel or convective medium [21]. However, while the previous study demonstrated the concept of OoO curing along with degree-of-cure (DoC) comparisons, mechanical and physical properties of OoO-cured composites have yet to be comprehensively evaluated, particularly properties dominated by interlaminar failure, a key area to evaluate for laminated composites [22]. To our knowledge, the direct comparison between OoO and traditional curing from an energy consumption analysis has not been reported in the extant literature. In the current study, we compare the OoO curing vs. oven curing using an OoA prepreg system, and find that the OoO curing enables highly efficient manufacturing of composites while preserving the mechanical properties, particularly interlaminar strength, equivalent to the conventional oven method.

Fig. 1a illustrates the overview of the conventional oven vs. the OoO curing process. Conventional oven curing processes as well as autoclaves that use convective heating require the entire vessel volume to be heated, regardless of the geometry of the component. Therefore, as shown in Fig. 1b, the electrical power for resistive heating should pass through several thermal barriers such as heat loss to the environment, the gas medium (here, air), and heating of vacuum bagging and cure materials to heat up a laminate. As a consequence, the energy consumption increases dramatically as the size of the structure increases. In contrast, the OoO curing has no thermal barriers between the heater and laminate, and thus transfers the heat via direct conduction because the CNT heater is installed on a surface of a laminate. Since the heat loss to the environment is connected to the heater in parallel, thermal insulation can suppress the heat loss, enabling most of electrical power to go into the laminate from the heater. Additionally, because the CNT film has extremely low thermal mass due to its low density (~25 gsm), the electrical power can increase the temperature of a laminate immediately.

2. Material and methods

The characteristics of the OoO curing process were explored by tracking thermal responses and electrical power consumption during a cure cycle. To compare the mechanical and physical properties of OoO-cured composites with those of oven-cured composites, degree of cure analysis, short beam shear test, dynamic mechanical analysis, and double-edge notch tensile testing were performed.

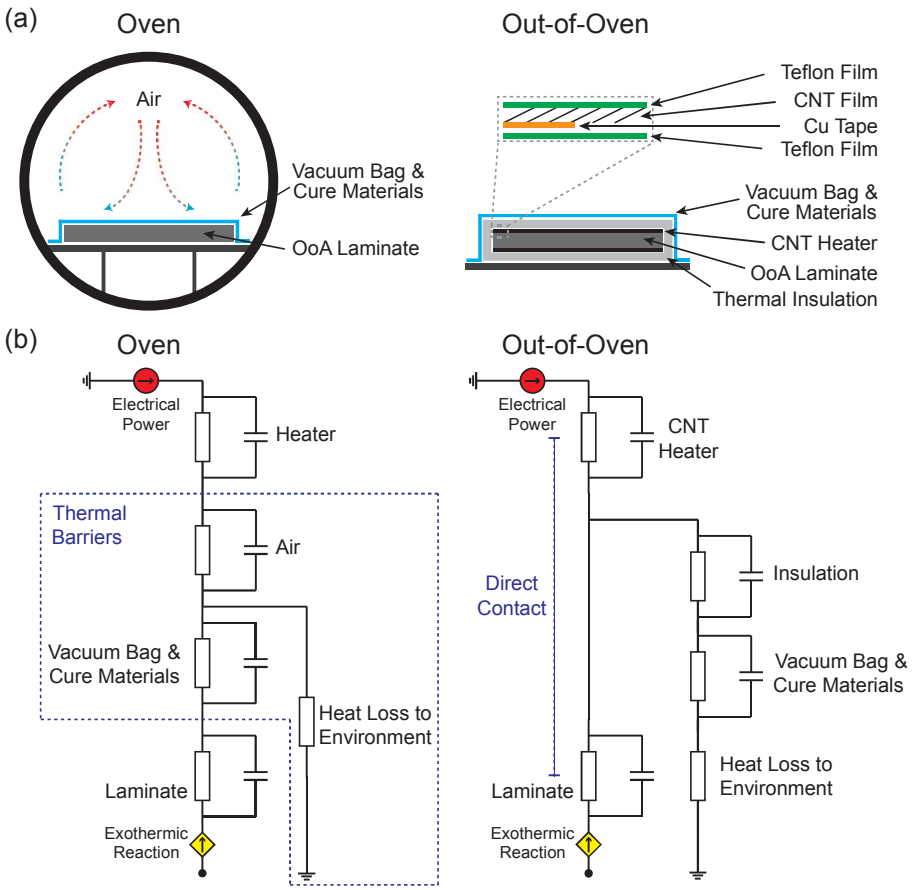

Fig. 1. Comparison of oven and out-of-oven (OoO) manufacturing process for out-of-autoclave laminate curing: (a) Overview of the physical differences between oven and out-of-oven process. (b) Comparison of thermal equivalent circuit model of oven and out-of-oven process. The circuits are symmetric with respect to the laminate. Note that the OoO process provides direct conductive heat transfer to the laminate, whereas the oven process passes through thermal barriers including the oven medium (air), vacuum bag, and cure materials.

2.1. Composite fabrication and processing

In this study, Hexcel IM7/M56 OoA aerospace-grade unidirectional (UD) carbon fiber prepreg was used [23], which is designed to be processed with a vacuum-bag-only curing method. The prepreg is nominally 394 gsm, and nominal cured ply thickness of this prepreg was 253 μm with a target of 58.8% V_f of carbon fiber in each ply. Considering the Standards used for the various experiments, and the field of view of synchrotron X-ray for *in-situ* tensile tests, eight plies (nominal laminate thickness of 2.02 mm) were used for the laminates quasi-isotropic layup of $[0/90/\pm45]_S$. Hexcel AS4/8552 unidirectional prepreg properties were used for the comparison of energy consumption, because the ANSYS Composite Cure Simulation (ACCS) provides the full engineering data of Hexcel AS4/8552 UD prepreg such as thermal conductivity, the exothermic heat of reaction for the cure modeling. The 16 plies of AS4/8552 UD prepreg were stacked up to match to the nominal thickness of the laminates comprised of IM7/M56 prepreg; the nominal cured ply thickness of AS4/8552 UD prepreg was 0.130 mm, giving a nominal laminate thickness of 2.08 mm, very close to the IM7/M56 nominal thickness of 2.02 mm. As a resistive heater, a commercialized CNT film, Veelo HEAT from General Nano LLC. [24], was utilized for this work. The CNT film was composed of randomly oriented multi-walled CNTs, and was ~40 μm thick, with an areal density of ~25 gsm and an isotropic sheet resistance of ~5 $\Omega/\square$.

For the oven curing process, the recommended vacuum bagging procedure from the prepreg manufacturer was followed [23,25]. To ensure the removal of air trapped during the hand lay-up process, vacuum debulking was performed on the full laminate at room temperature for 6 h. After the debulking process, the rounded laminate edges were trimmed to ensure the laminate is re-breathable, a step necessitated by the OoA formulation of the prepreg, following manufacturer recommendations. Once a vacuum bag was prepared for the cure, the laminate and cure materials was placed in a gravity convection oven (i.e., Lindberg/Blue M, GO1350A) for curing. During the cure cycle, the recommended curing condition in the technical data sheet was followed for each prepreg system. Both prepreg systems are designed to have the same temperature for the thermal process as follows: cure temperature of 110 °C with a hold time of 60 min, and post cure temperature of 180 °C with a hold time of 120 min; ramp rate at 3 °C/min.

For OoO curing, the cure setup was modified as a form of conductive curing, similar to the previous study (See Fig. S1 for the modified vacuum bagging setup with a one-sided heater). In particular, thermal insulating blocks (i.e., MICROSIL Microporous Insulation from ZIRCAR Ceramics Inc.) were installed to reduce heat loss to the environment. In addition, because one of the main goals of this study was to compare the physical properties of oven vs. OoO curing, a Guaranteed Nonporous Teflon (GNPT) film was inserted between the heater and the surface of the laminate such that the OoO heater can be easily peeled off after cure. Such removal of the heating element is different from the previous study using a CNT nanocomposite heater; a conductive CNT polymer nanocomposite was permanently attached to the surface of the laminate with a surfacing film in the prior work [21,26]. During an OoO cure cycle, a DC power supply was connected to the two copper tape electrodes of the heater to control the input voltage to follow the specific cure cycle [21,26]. For the feedback control, the input voltage was used for the system input, and the temperature of a CNT heater was the system output. Temperature of the CNT heater was measured via a thermocouple (OMEGA Engineering fast-response K-type). The input voltage was controlled to make the temperature error less than 0.1 °C, while following the designated cure cycle. The vacuum bagging setup was placed on a lab bench. Input voltage, current, and power consumption were recorded using digital multimeters embedded in the power supply (B&K Precision DC power supply 9201).

2.2. Characteristics of oven and out-of-oven curing

To evaluate the energy consumption of an oven process and OoO process, the power consumption was measured during a cure cycle and compared with the model of the multi-physical curing process by ACCS. The transient thermal analysis was conducted to capture thermal responses within a laminate such as a temperature and heat flux. As mentioned above, a quasi-isotropic laminate comprised of unidirectional layers of Hexcel AS4/8552 prepreg in a $[0/90/\pm45]_{2S}$ layup was used for finite element cure modeling due to the full accessibility of engineering data. Each ply was modeled with ten meshes to obtain results through the thickness of the laminate. Note that the cure simulation was conducted in 1D, while the experiment was under 3D.

For an oven process, a gravity convection oven was used in the experiment and the model. The dimension and engineering data such as the amount of heat loss to the environment were adopted to the model from the technical data sheet of the manufacturer [27]. The thermal analysis assumed that a vacuum bag and cure materials are surrounded by the heated air during a cure cycle. The power consumption was acquired by calculating the electrical power of the heating elements. The convective heat transfer coefficient was set at 15 W/m°C at the surface of the vacuum bag, and the dry air of an oven was modeled as a lumped capacitance model. The heat flux from a laminate due to the exothermic reaction of the thermoset was included in the calculation. In the experiment, the electrical power consumption was measured directly at the receptacle via a current probe (FLIR TA72). For the OoO process, we assumed that the temperature of a cure cycle was applied to the surface of a laminate because the CNT heating component is mounted directly on a surface of a laminate. The engineering data of thermal insulation (density of 230 kg/m^3, specific heat of 800 J/kg°C, and thermal conductivity of 0.019 W/mK at 20 °C to 0.023 W/mK at 200 °C with the assumption of linearity) was introduced for the model. The experimental electrical power consumption was obtained by measuring the input voltage and current into the CNT heater mounted on laminate via a DC power supply.

2.3. Degree of cure analysis

After the curing using the oven and OoO methods, differential scanning calorimetry (DSC) was conducted using a Discovery DSC (TA instruments) to evaluate the degree of cure (DoC) of the laminate. The dynamic DSC run was performed by scanning the heat flow from 40 °C to 300 °C at 5 °C/min ramp rate, based on ASTM D7028. The DoC was estimated by comparing the area of the exothermic peak observed in the DSC curve of the heat-processed laminate, also known as the heat of reaction, to that of an uncured laminate. The DSC specimens were taken from each layer of a laminate so that the through-thickness variance of the DoC could be assessed, particularly given the one-sided nature of the OoO curing. For the DSC testing, eight plies of 60 mm × 50 mm IM7/M56 laminae were stacked unidirectionally by hand lay-up technique, and release films were introduced to both the left and right end of the laminate in between top, middle, and bottom layers for easy separation after curing [21,28]. The release film prevents resin flow between layers. The procedures for oven and OoO curing followed the same procedures described in the section above.

2.4. Short beam shear testing

The short beam shear (SBS) test was conducted based on ASTM standard D2344, which is also consistent with DIN EN2563, and is the simplest test for interlaminar shear strength (ILSS). The dimension of a specimen was nominally 12 mm × 4 mm × 2 mm (L × W × t), and these specimens were taken from the 120 mm × 120 mm unidirectional laminates comprised of 8 plies of IM7/M56 prepreg. Small angles (±2°) between the plies were introduced intentionally to avoid fiber nesting [29]. The cut laminate edges were polished with 800, 1200, and 2400 grit sandpapers to avoid rough or uneven surfaces which may result in pre-cracks following the Standard. As prescribed in the ASTM standard D2344 [30], a three-point bend fixture with a loading nose of 6 mm, supports of 3 mm diameter steel cylinders, and the span length of 8 mm was utilized. During the tests, the force applied to the specimen was monitored at a rate of cross head movement of 1.0 mm/min applied by a Zwick/Roell Z010 mechanical testing machine. The short-beam strength was then calculated using Eq. (1) as follows:

$$\sigma_{SBS} = 0.75 \times \frac{P_f}{w \times t} \tag{1}$$

where P_f, w, and t are the load at the failure observed during the test, the width, and the thickness of the specimen, respectively.

2.5. Dynamic mechanical analysis (DMA)

The specimen dimensions and testing procedure were carried out based on the ASTM standard D7028. The Dynamic Mechanical Analyzer used for the characterization of the composite laminates was a TA Q800 DMA (TA Instruments). All DMA tests were conducted using a three-point bending fixture with a span of 50 mm, which is ideal for composite materials due to its simpler stress distribution than that induced in a single or double cantilever configuration and measurable strain for high modulus materials [31]. For DMA tests, an 8-ply unidirectional laminate of 120 mm × 120 mm was cured by oven and OoO process, respectively. In the same manner, the small angle between plies was used to prevent the fiber nesting. Four specimens of 60 mm × 12 mm × 2 mm (L × W × t) taken from each oven-cured and OoO-cured laminate were tested in the temperature range from 40 °C to 300 °C at 2 °C/min heating rate, maximum strain of 50 μm, and multi-frequency sweep of 1, 3.2, 10, 30 Hz. The storage modulus, loss modulus, and tan delta were obtained via DMA test, and the glass transition temperature was determined from the storage modulus curve. Among three different ways to determine glass transition temperature, the tan delta curve was additionally used for determination of glass transition temperature to conduct the most refined comparison of the oven-cured and the OoO-cured laminate with its clearness, even though the storage modulus curve is widely used because of its conservativeness [31]. The estimation of the activation energy is most likely to be consistent when the glass transition temperature is determined by the tan delta peak [31–34]. The multi-frequency sweep results were analyzed to estimate the activation energy of the glass transition relaxation as an additional comparator of the oven vs. OoO manufacturing methods. The monitoring of the activation energy is correlated to the modulus and compliance of a composite at the end of the service life, and therefore is useful in assessing environmental exposure and aging of the material [32,34–37]. The estimation of the activation energy is based on the effect of temperature on the frequency of molecular conformational changes in polymers [37,38]. Such phenomenon can be explained by the Arrhenius relationship: the increase in frequency leads to the shift of the tan delta curve toward a higher temperature. The activation energy can be estimated by obtaining the slope of the ln$f$ vs. $\frac{1}{T_g}$ with Eq. (2) as follows [31]:

$$\Delta H = -R\frac{d(\ln f)}{d\left(\frac{1}{T_g}\right)} \tag{2}$$

where ΔH is the activation energy (kJ/mol) for the glass transition relaxation, R is the universal gas constant(J/mol K), f is the testing frequency (Hz), and T_g is the glass transition temperature in Kelvin (K).

2.6. Double-edge notch tensile (DENT) test

To compare the tensile strength and the failure progression of OoO-cured laminates with those of oven-cured laminates, *ex-situ* and *in-situ* tensile testing with double-edge notch specimens were conducted. For this test, a quasi-isotropic laminate (IM7/M56, $[0/90/\pm45]_S$) of 120 mm × 120 mm was cured by each manufacturing method. The 1 mm-radius double-edge notches were introduced into the 36 mm-long and 4 mm-wide specimens using an abrasive waterjet so that the failure occurs within the X-ray field of view during *in-situ* tensile testing [39,40].

The CT5000 5kN *in-situ* tensile stage for μXCT (Deben UK Ltd.) was used as a load frame for both *ex-situ* and *in-situ* tensile testing. All tensile testing with the *in-situ* stage was conducted under 0.3 mm/min motor speed. The ultimate tensile strength (UTS) of each specimen was calculated with the area at the notch and the maximum load at failure. To evaluate the failure mode and progression, the specimens were scanned via *in-situ* synchrotron X-ray computed tomography (SRCT) prior to tensile loading and followed by scans at incrementally increasing stress range from 30% to 100% UTS in steps of 10%. The *in-situ* experiment was performed at the beamline 2-BM of the Advanced Photon Source (APS), Argonne National Laboratory (ANL). An isotropic voxel size of 1.3 μm was acquired with the X-ray beam energy of 22.7 keV and a 5× objective lens. For each scan, 1500 2D projections were captured while a specimen was rotated in 180° via 2560 × 2160 PCO.Edge 5.5 sCMOS camera. The exposure time for each projection was 100 ms, and the projection radiographs were reconstructed using TomoPy [41], an open source Python based toolbox, and a reconstructed 3D volumes were analyzed with the commercial visualization software, Avizo (FEI), to segment the features of interest such as matrix damage.

3. Results and discussion

Thermophysical and mechanical testing results are discussed for both curing methods, followed by a failure progression study utilizing *in-situ* synchrotron computed tomography.

3.1. Characteristics of oven and out-of-oven curing

Fig. 2 shows the cure simulation and experimental results for the oven and OoO curing process for the 2 mm-thick 60 mm × 50 mm laminate. As presented in Fig. 2a, the oven process showed an expected transient temperature response on the laminate surface due to the convective heat transfer, whereas the OoO process had an immediate response by conductive heat transfer. As mentioned in the Introduction, the convection coefficient in the heating vessel varies greatly due to uncontrolled factors that influence gas flow dynamics, resulting in temperature gradients in a laminate [18–20]. Furthermore, if several parts are cured simultaneously in a heating vessel, part-to-part variation may occur. However, because the OoO process directly controls the temperature of each part, OoO curing has the potential to reduce part-to-

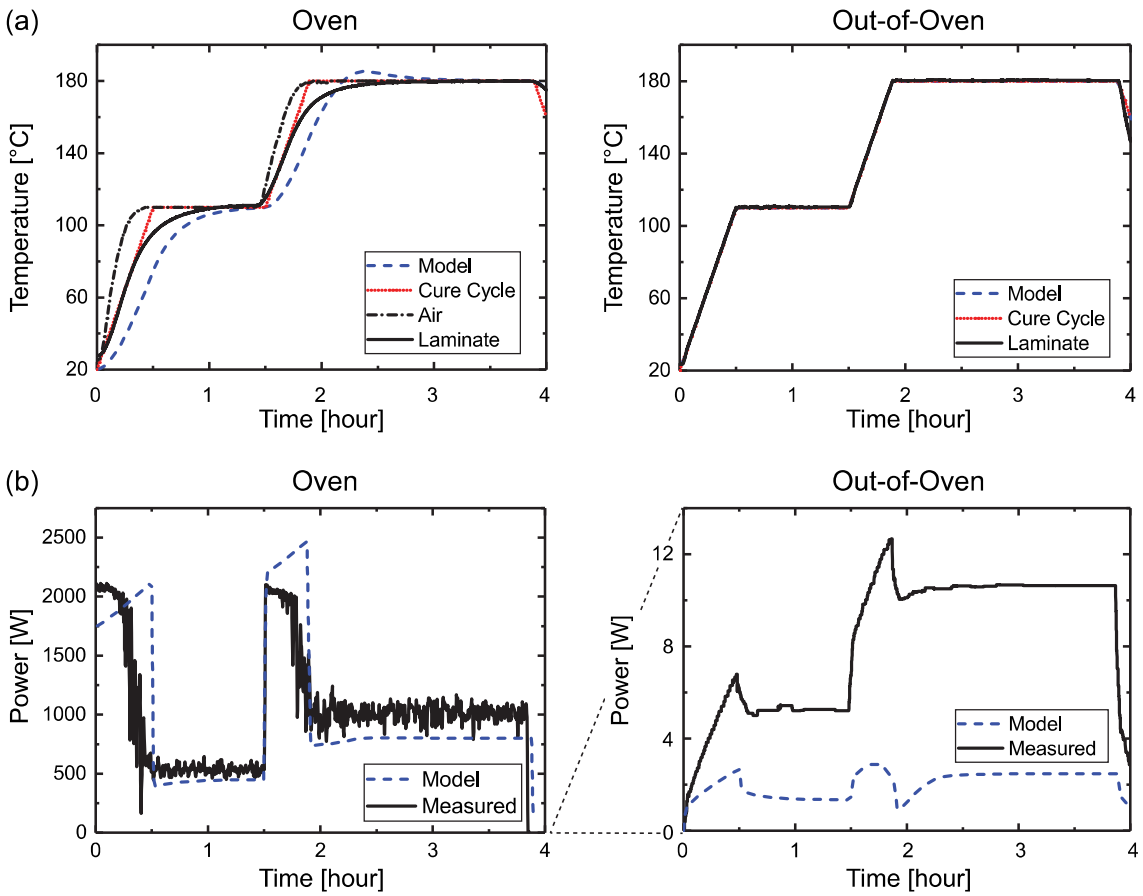

Fig. 2. Comparison of temperature profile and power consumption during oven and out-of-oven curing: (a) Temperature profile, and (b) Power consumption. The out-of-oven curing showed a reduction in input electrical energy by two orders of magnitude. Note the difference in scale between the oven and OoO power axes.

part variation due to thermal history during curing.

A clear difference between the oven and OoO process arises from the two orders of magnitude reduction in energy consumption during the curing cycle. An oven having the ideal size for composite parts is rarely available in practice, and the part volume needs to be kept low in the heating vessel to ensure effective convection and uniform heating, which are critical for part quality and dimensions [42]. Therefore, it is not uncommon to cure parts to have a volume much less than the volume of the oven or autoclave. In our oven curing experiments, the part-to-oven volume is 0.1%, typical of research autoclaves, and of the same order as that of composite production autoclaves, e.g., curing of an aerospace wing shell (which should be closely optimized to the autoclave used, has a part-to-autoclave volume ration of 0.4% (3.54 m^3 part, and 896 m^3 autoclave) [43–45]. Thus, the energy savings due to the conductive OoO curing method of two orders of magnitude for the oven considered herein is relevant at the commercial scale. It should be noted that the energy savings measured herein is also in agreement with simple models (based on volume considerations) presented previously [21].

The lower images of Fig. 2b show the power consumption of each manufacturing process during a cure cycle. In the case of oven curing, most of the power consumption was used to raise the temperature of the medium gas (i.e., dry air) inside the oven and to maintain the temperature against heat loss to the environment. Since the amount of heat loss to the environment provided in the technical data sheet was included in the convection oven model, the power consumption of the model was in good agreement with the experimental results. During the ramp-up period, power consumption of ~2.1 kW was observed, and ~500 W and ~1 kW were consumed at the 110 °C and 180 °C hold steps, respectively. In contrast, the OoO process exhibited a maximum power consumption of ~12.5 W, two orders of magnitude lower than the oven curing process. The total energy consumption during the entire curing cycle was 13.7 MJ for the oven and 118.8 kJ for the OoO process, respectively - two orders of magnitude less for the OoO vs. the oven cure. Since the OoO curing process is adjusted proportionally to the surface area of the part, the energy savings are expected to be particularly prominent in aspect ratios commonly found in wind, aerospace, and other applications where parts are often long and narrow such as a wing and fuselage. Note that the model captured the slight reduction of electrical power at the early stage of the post-cure cycle; a valley in the power plot was observed at ~1.9 h (See Fig. 2b) due to the exothermic heat of reaction.

Additionally, we conducted the OoO curing experiment with a 20 mm-thick laminate comprised of 160 plies of 60 mm × 50 mm to evaluate if the exothermic heat of reaction of the thermoset polymer affects the power consumption during curing. See Section S3 in the Supplementary Materials for experimental details and results. Oven curing exhibited temperature overshoots of ~35 °C within the whole laminate at the early stage of a post-cure cycle due to the exothermic heat of reaction. Relatively, OoO curing showed a decreased magnitude of the overshoot of ~25 °C and ~10 °C at the center and a surface of a laminate, respectively. The results suggest that OoO process helps following an intended cure cycle, resulting in the final thermal and mechanical properties close to the targeted

values. We observed that the exothermic heat of reaction from a laminate resulted in the ~20 min period in the early stage of post-cure cycle where any electrical power input was not required (See Fig. S3 in the Supplementary Materials). Such a phenomenon indicates the possibility of further energy saving by recycling the heat of reaction of a laminate to cure itself.

3.2. Thermophysical properties

DoC via DSC and characterizations from DMA are used to compare the thermophysical attributes of the OoO to oven curing. Three DSC specimens were prepared from the top (the 1st ply adjacent to the CNT heater), the center (the 4th ply), and the bottom ply (the 8th ply), to establish through-thickness spatial trends in DoC. The mean value of the heat of reaction acquired from three uncured prepreg was used for the calculation of DoC. The expected range of DoC for oven manufacturing for this material is in the range of 90–95% (per the manufacturer), which is typical of most oven and autoclave processed aerospace-grade composites. As presented in Fig. 3, the DoCs of both oven and OoO process are in the targeted range. To determine whether means of oven and OoO curing are statistically different, the one-way analysis of variance (ANOVA; Welch's ANOVA [46]) was conducted. The ANOVA is used throughout the discussion to compare oven and OoO curing, and a p-value less than 0.05 is required to establish a statistical difference with 95% confidence. The DoCs of an OoO-cured laminate showed no statistical difference from those of an oven-cured laminate. There was no significant spatial variation in both cases. The previous study without thermal insulation found that the DoC of the laminate strongly depends on the thermal distribution within a laminate [21]. In particular, the DoC of the laminate correlates to the surface temperature of the CNT heater, and the DoC decreased in the through-thickness direction away from the heater due to the thermal losses as the distance from the CNT heater increases. Therefore, the results of this study indicate that simple thermal insulation can further improve the in-plane thermal distribution and minimize through-thickness DoC trends. Overall, a one-sided CNT heater on a 2 mm-thick laminate is enough to obtain the equivalent thermal properties of oven-cured laminates.

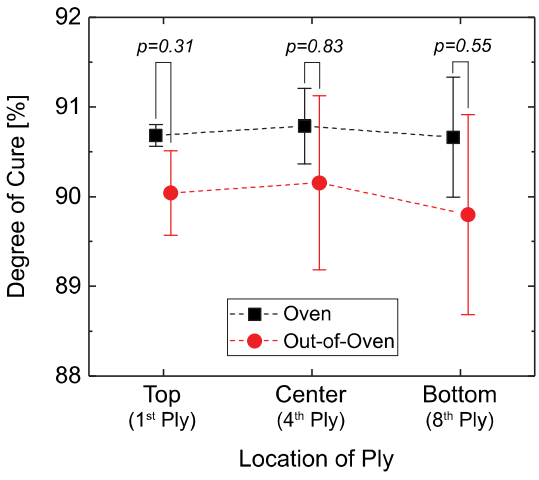

Fig. 3. Comparison of degree of cure as evaluated spatially via differential scanning calorimetry (DSC) at the top, center, and bottom plies of 8-ply laminate for oven and out-of-oven curing. Note that the whiskers represent the standard error. Data is offset slightly on the x-axis (ply location) for visualization. Note that in the out-of-oven curing process, the heater is in contact with the top ply (the 1st ply). p-values of 0.31, 0.83, and 0.55 indicate that there are no significant differences between the oven and out-of-oven curing process.

The results from DMA curves such as the storage modulus, loss modulus, and tan delta, altogether suggest that oven-cured and OoO-cured specimens exhibit the same dynamic mechanical responses. See Fig. 4a for the representative storage modulus, loss modulus, and tan delta curve from DMA tests on the specimens at the testing frequency of 1 Hz. Fig. 4b exhibits the storage modulus and loss modulus at 100 °C as well as the magnitude of the tan delta peak. The results of the p-value in all three curves ($p = 0.84$ for the storage modulus; $p = 0.25$ for the loss modulus; and $p = 0.18$ for the tan delta peak) suggest that there is no significant difference in the curves of oven-cured and OoO-cured specimens. The glass transition temperature determined by the storage modulus curves ($T_{g,s}$) and tan delta curves ($T_{g,t}$) at 1 Hz frequency, and estimated activation energy from the multi-frequency sweeps at 1, 3.2, 5, and 30 Hz, are summarized in Table 1. For the estimation of activation energy, $T_{g,t}$ was used as it is considered the most accurate [31–34]. The oven-cured and OoO-cured specimens exhibited the same $T_{g,t}$ and $T_{g,s}$ of ~227 °C and ~205 °C, respectively. It should be noted that the manufacturer reported $T_{g,s}$ of 204 °C [23] is very close to the values measured here. It is known that the glass transition temperature measured by DMA curves may vary by up to 25 °C depending on the parameter and methodology for testing [34,47]. The oven-cured and the OoO-cured specimens exhibit statistically no difference in $T_{g,s}$, $T_{g,t}$, and activation energy as shown above and in Table 1. Therefore, the DMA tests indicate that the oven and OoO curing provide the comparable dynamic properties of the polymer as expected.

3.3. Mechanical testing

Here we explore the results of SBS and double-edge notch strength testing to further assess any differences in OoO vs. oven curing as well as the morphology of the fabricated laminates. Fig. 5 presents synchrotron radiation μCT images of the oven-cured and OoO-cured specimen. As presented, both specimens did not show any detectable void under a high resolution scan (voxel size of 1.3 μm). There was no morphological differences noted between the oven and OoO specimens. In the SBS test, 14 specimens were tested for each curing process. In both cases, it was observed that the failure proceeds sequentially as: (1) plastic deformation as an indentation at the loading nose, followed by (2) interlaminar shear failure (as defined in the Standard D2344 as a valid test), which resulted in the type of load-deflection of each case as shown in the inset of Fig. 6. The first failure corresponds to indentation and/or crushing at the loading nose, and the maximum load (second failure) occurs due to the interlaminar shear failure. It is known that the short-beam strength may not directly indicate the interlaminar shear strength of the laminate due to its complex stress distribution, and that the failure can be a combination of different failure modes such as discrete and irregular interlaminar shear, tension, compression, and plastic deformation [48]. However, it is generally accepted that SBS testing can be used for comparison and as a screening tool for composite laminate properties with a description of the failure mode [49,50]. Fig. 6 exhibits the short-beam strength of oven-cured and OoO-cured specimens in a boxplot. Note that the boxes represent the interquartile range for each group; the line in the middle of each box represents the median, and the whiskers represent the minimum and maximum datum; the outlier was determined by the Tukey's fences [51]. Since the specimens failed in complex modes (i.e., indentation and interlaminar shear), the first failure load and the maximum load observed during the test were both analyzed for the short-beam strength. The oven-cured specimens showed the short-beam strength of 99.22 MPa (SE = 0.70 MPa) at first failure and 109.11 MPa (SE = 0.70 MPa) at the maximum load. The OoO-cured specimens showed the short-beam

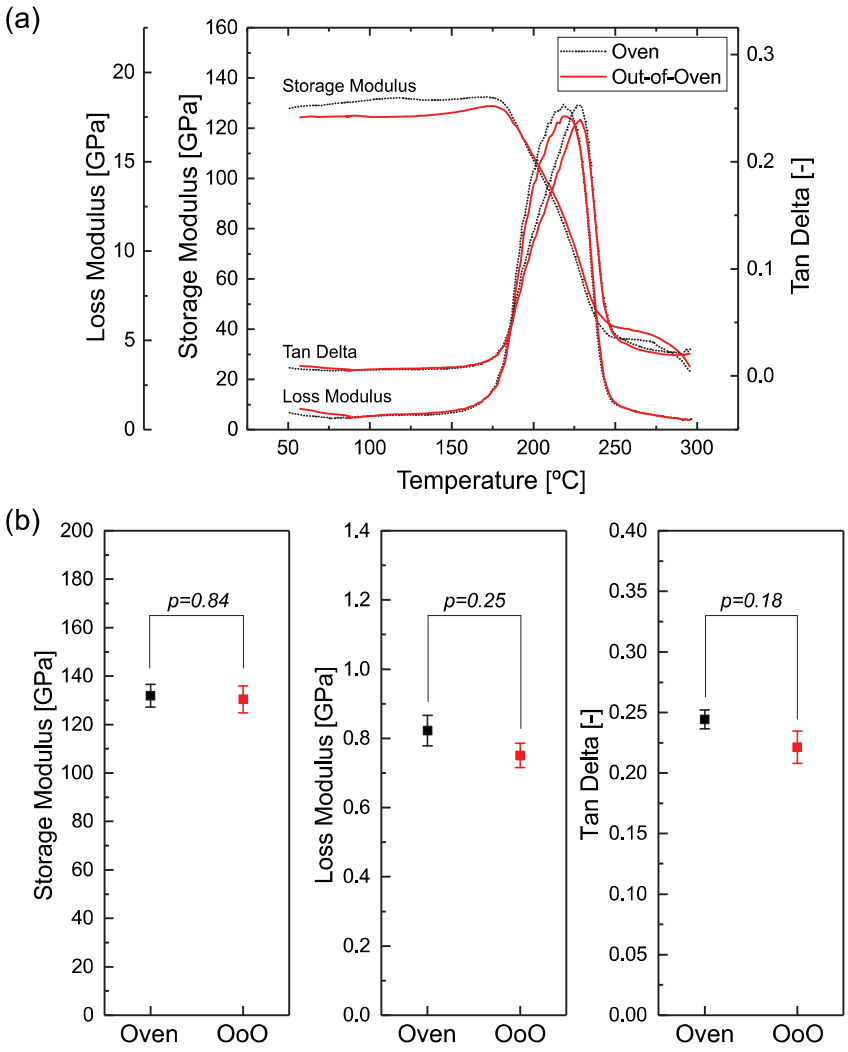

Fig. 4. DMA results. (a) Representative storage modulus, loss modulus, and tan delta curve from DMA tests at the testing frequency of 1 Hz for oven and out-of-oven specimens. (b) Storage modulus and loss modulus at 100 °C, and the magnitudes of tan delta peak of the oven and the out-of-oven specimens. Note that the whiskers represent the standard error. *p*-values of 0.84, 0.25, and 0.18 indicate that there are no significant differences between the oven and out-of-oven curing process.

Table 1
Glass transition temperature and activation energy of relaxation of the oven and the out-of-oven specimens. Note that the glass transition temperatures obtained from the storage modulus curves and tan delta curves correspond to $T_{g,s}$ and $T_{g,t}$, respectively. *p*-values of 0.99, 0.75, and 0.68 indicate that there are no significant differences between the oven and out-of-oven curing process.

Specimen Number	$T_{g,s}$ (°C)		$T_{g,t}$ (°C)		Activation Energy (kJ/mol)	
	Oven	OoO	Oven	OoO	Oven	OoO
1	207.38	204.27	227.19	226.44	549.71	553.71
2	203.97	206.39	226.63	228.50	553.36	698.34
3	204.43	205.85	227.44	228.01	556.35	557.35
4	206.94	206.25	227.72	228.97	694.59	629.12
Average	205.68	205.69	227.25	228.01	588.50	609.63
Standard Error	0.86	0.48	0.23	0.56	35.39	34.29
p-value	0.99		0.75		0.68	

strength of 100.40 MPa (SE = 1.93 MPa) at the first failure and 110.62 MPa (SE = 1.10 MPa) at the maximum load. Therefore, the oven-cured and the OoO-cured specimens showed similar short-beam strength both at first failure and the maximum load. The ANOVA was again conducted to determine whether means of oven and OoO are statistically the same for the short-beam strength conditions. As presented, the results of the *p*-values in both short-beam strength cases ($p = 0.74$ for the first failure and $p = 0.29$ for the maximum load) suggest that the means of short-beam strength values of oven-cured and OoO-cured specimens are not significantly different from each other. Therefore, we conclude that oven-cured and OoO-cured specimens have the same strength at each failure mode as well as the same sequential order of failure mode. Given the correct mode of interlaminar failure at the maximum

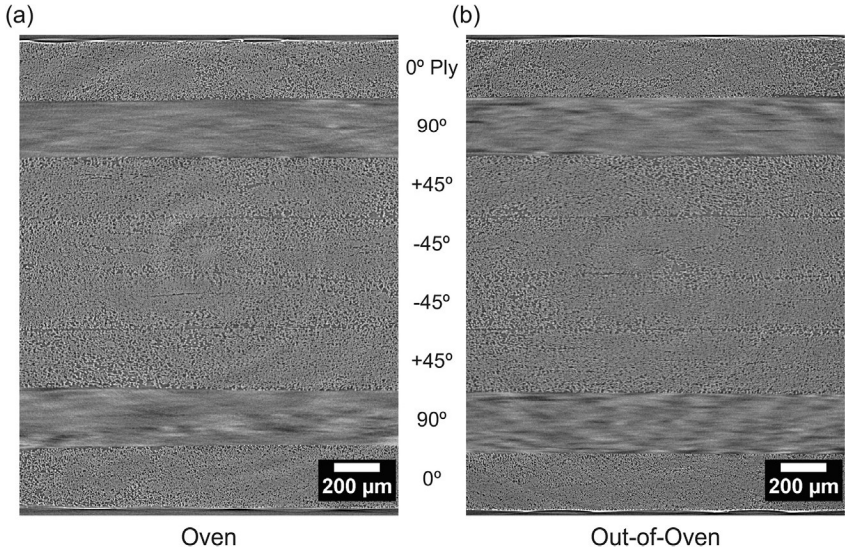

Fig. 5. Representative synchrotron radiation μCT image of (a) an oven specimen, and (b) an out-of-oven specimen. Note that both laminates were comprised of a quasi-isotropic ($[0/90/\pm45]_S$) lay-up sequence. There are no observed voids or morphological differences in the cross sections.

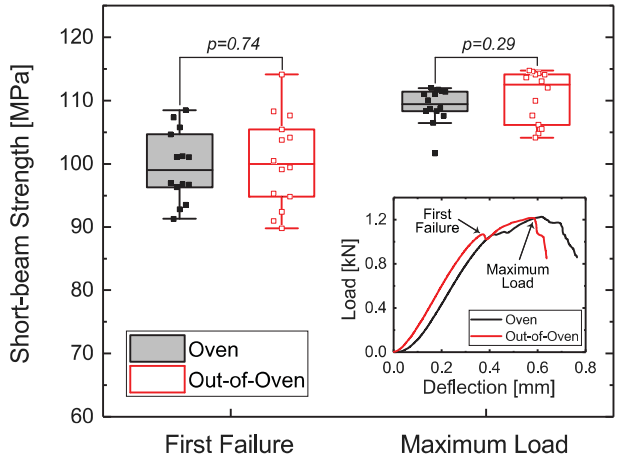

Fig. 6. Short-beam strength of oven and out-of-oven specimens. Note that the boxes represent the interquartile range for each group; the line in the middle of each box represents the median, and the whiskers represent the minimum and maximum datum; the outlier was determined by the Tukey's fences [51]. The inset figure shows representative load-deflection curves for the two types of curing as discussed in the main text. Due to the initial load drop ("first failure"), both the first failure and maximum load were used for the determination of the strength. Considering *p*-values, the means of short-beam strength values of oven-cured and OoO-cured specimens are not significantly different from each other.

load, we conclude that this is the more important comparison as this stress is the SBS. It should be noted that the manufacturer reported ILSS of 98.6 MPa [23], very close to the lower values measured here. ILSS has many measures with SBS considered more qualitative and comparative, rather than a true measure of ILSS.

Fig. 7a shows the UTS results for double-edge notch specimens of the oven-cured and the OoO-cured laminates. As presented, the oven-cured specimens showed a DENT UTS of ~562.04 MPa (SE = 8.09 MPa), while the OoO-cured specimens performed the UTS of ~566.68 MPa (SE = 10.54 MPa). Given that the manufacturer reported IM7/M56 showed comparable fiber-dominated strengths as IM7/8552 [52], the measured DENT UTS can be compared with the strengths of IM7/8552 as follows: the DENT UTS is expected to be considerably lower than the unnotched tensile strength, and similar to the open hole tensile strength, given an equivalent stacking sequence. It was reported that the specimens comprised of IM7/8552 quasi-isotropic layup ($[45/0/-45/90]_{2S}$) have unnotched tensile strength of 717.12 MPa and open hole tensile strength of 458.66 MPa [53]. Since the DENT UTS of ~564 MPa were in between the unnotched tensile and open hole tensile strength, they are considered to be in a reasonable range. Similarly, the ANOVA was applied to evaluate whether means of oven and OoO are statistically the same. The significant level is 0.73, which is above 0.05, therefore, there is no statistically significant difference in the means of UTS value between oven-cured and OoO-cured specimens.

Fig. 7b presents the 3D rendering of damages at 0%, 50%, 70%, and 90% UTS. During *in-situ* tensile testing, three major damage mechanisms have been observed in both oven and OoO specimens as followed: intralaminar splits in 0° ply, transverse ply cracks in 90° ply, and intralaminar cracks in ±45° plies. Considerable amounts of cracks were observed at 70% UTS, while crack initiations occurred at 50% UTS from the notches in both cases. The oven-cured and OoO-cured specimens showed the same crack progression trend: most of cracks in ±45° plies were formed after the crack formation in 0° ply and 90° ply. Thus, we conclude that the tensile strengths of oven-cured and OoO-cured specimen were statistically same and the crack progression occurred in the identical manner. Because of the limitation of qualitative evaluation of the crack progression, future work on the crack opening displacement and the volume of the cracks will provide a quantitative comparison of oven and OoO specimens.

4. Conclusion

In summary, we examined the characteristics of the out-of-oven curing process using a carbon nanotube film as a heating element, compared to that of a conventional oven composite curing process, for an aerospace-grade out-of-autoclave (OoA) formulated unidirectional carbon fiber advanced composite prepreg system. We further evaluated the thermophysical and mechanical properties of the processed out-of-autoclave composites. Results suggest that there is no significant difference between the out-of-oven curing and oven curing in the degree of cure analysis, short beam shear, dynamic mechanical analysis, and double-edge notch tensile test;

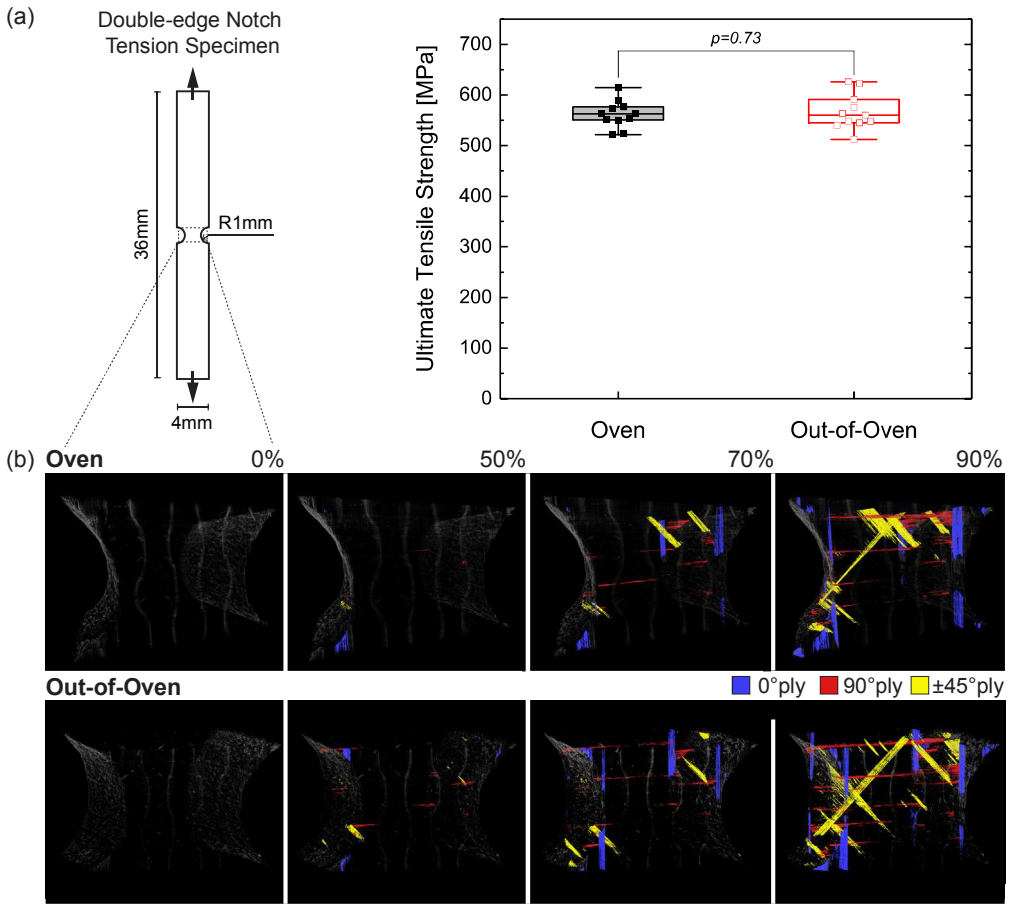

Fig. 7. Results of double-edge notch tensile *ex-situ* and *in-situ* testing for oven and out-of-oven curing. (a) Ultimate tensile strength of double-edge notch specimens, and (b) 3D rendering of damage (matrix cracks) at 0%, 50%, 70%, and 90% of the mean ultimate tensile strength. Note that the boxes represent the interquartile range for each group; the line in the middle of each box represents the median, and the whiskers represent the minimum and maximum datum. A *p*-value of 0.73 indicates that there is no significant difference between the oven and out-of-oven specimens. The oven and the out-of-oven specimens demonstrated equivalent damage progression.

therefore, the out-of-oven curing can achieve the equivalent thermal and mechanical properties of out-of-autoclave composites, as the conventional curing method. Moreover, the out-of-oven composite curing process provides a significant reduction in electrical energy consumption by two orders of magnitude (from 13.7 to 0.12 MJ). The modeling of each manufacturing technique showed good agreement with electrical power consumption during a cure cycle, including reduction in electrical power consumption. Next-generation composite manufacturing may overcome the limitations of the conventional composite manufacturing process with several advantages as follows: (1) Removal of size and shape constraint on composite components using a scalable conductive heating element, (2) on-site curing and/or repair, (3) high accessibility to the composite manufacturing facilities, and (4) cost savings on manufacturing by efficient thermal processing. Considering that one of the benefits of the out-of-oven process is a rapid ramp rate, future work should explore the further reduction of energy consumption and the evaluation of thermophysical and mechanical properties of the out-of-oven-cured composites fabricated by a rapid-heating-enabled cure cycle.

Acknowledgements

This work was primarily supported by Airbus, and partially supported by Airbus, Embraer, Lockheed Martin, Saab AB, Hexcel, Saertex, TohoTenax, and ANSYS through MITs Nano-Engineered Composite aerospace Structures (NECST) Consortium. This work made use of the facilities at the Institute for Soldier Nanotechnologies at MIT, supported (in part) by the U.S. Army Research Laboratory and the U.S. Army Research Office through the Institute for Soldier Nanotechnologies, under contract number W911NF-13-D-0001. This research used resources of the Advanced Photon Source, a U.S. Department of Energy (DOE) Office of Science User Facility operated for the DOE Office of Science by Argonne National Laboratory under contract number DE-AC02-06CH11357. The authors would like to thank Pavel Shevchenko at the 2-BM beamline of the Advanced Photon Source at Argonne National Laboratory. Authors are grateful to the MIT co-workers at the beamline; Reed Kopp, Nathan Fritz, and Travis Hank. J.L. acknowledges support from Kwanjeong Educational Foundation. The authors kindly thank Hexcel for donation of the OoA prepreg.

Appendix A. Supplementary data

Supplementary data related to this article can be found at https://doi.org/10.1016/j.compscitech.2018.02.031

References

[1] F.C. Campbell Jr., Manufacturing Technology for Aerospace Structural Materials, Elsevier, 2011.
[2] H. Charles E, J. James, H. Starnes, S. Mark J, An Assessment of the State-of-the-art in the Design and Manufacturing of Large Composite Structures for

Aerospace Vehicles, Tech. rep, 2001.
[3] D. Abliz, D. Yugang, L. Steuernagel, X. Lei, L. Dichen, G. Ziegmann, Curing methods for advanced polymer composites - a review, Polym. Polym. Compos. 21 (6) (2013) 341–348.
[4] C. Joseph, C. Viney, Electrical resistance curing of carbon-fibre/epoxy composites, Compos. Sci. Technol. 60 (2) (2000) 315–319.
[5] J.W. Kim, G. Sauti, E.J. Siochi, J.G. Smith, R.A. Wincheski, R.J. Cano, J.W. Connell, K.E. Wise, Toward high performance thermoset/carbon nanotube sheet nanocomposites via resistive heating assisted infiltration and cure, ACS Appl. Mater. Interfaces 6 (21) (2014) 18832–18843.
[6] B. Mas, J.P. Fernández-Blázquez, J. Duval, H. Bunyan, J.J. Vilatela, Thermoset curing through Joule heating of nanocarbons for composite manufacture, repair and soldering, Carbon 63 (2013) 523–529.
[7] G. Gardiner, Out-of-autoclave prepregs: hype or revolution? High Perform. Compos. 19 (2011) 32–39.
[8] T. Centea, L.K. Grunenfelder, S.R. Nutt, A review of out-of-autoclave prepregs - material properties, process phenomena, and manufacturing considerations, Compos. Appl. Sci. Manuf. 70 (0) (2015) 132–154.
[9] L.K. Grunenfelder, S.R. Nutt, Air removal in VBO prepreg laminates: effects of breathe-out distance and direction, in: 43rd International SAMPE Tech Conference, 2011.
[10] B. Louis, K. Hsiao, G. Fernlund, Gas permeability measurements of out of autoclave prepreg MTM45-1/CF2426A, in: 54th International SAMPE Symposium and Exhibition, 2010, pp. 17–20.
[11] M. Wysocki, R. Larsson, S. Toll, Modelling the consolidation of partially impregnated prepregs, in: Proceedings of the 17th International Conference on Composite Materials, 2009, pp. 1–10.
[12] C. Ridgard, Out of autoclave composite technology for aerospace, defense and space structures, in: Proceedings of the SAMPE 2009 Conference, 2009.
[13] L. Repecka, J. Boyd, Vacuum-bag-only-curable prepregs that produce void-free parts, in: Proceedings of the SAMPE 2002 Conference, 2002, pp. 1862–1874.
[14] L.K. Grunenfelder, T. Centea, P. Hubert, S.R. Nutt, Effect of room-temperature out-time on tow impregnation in an out-of-autoclave prepreg, in: Composites Part a: Applied Science and Manufacturing vol. 45, 2013, pp. 119–126.
[15] L. Fahrang, G. Fernlund, Void evolution and gas transport during cure in out-of-autoclave prepreg laminates, in: Proceedings of the SAMPE 2011 Conference, 2011, pp. 1–15.
[16] T. Centea, S.R. Nutt, Manufacturing cost relationships for vacuum bag-only prepreg processing, J. Compos. Mater. 50 (17) (2015) 2305–2321.
[17] R.A. Witik, F. Gaille, R. Teuscher, H. Ringwald, V. Michaud, J.-A.E. Manson, Economic and environmental assessment of alternative production methods for composite aircraft components, J. Clean. Prod. 29-30 (2012) 91–102.
[18] P.F. Monaghan, M.T. Brogan, An overview of heat transfer for processing thermoplastic composites in autoclaves, Compos. Manuf. 2 (3–4) (1991) 233–242.
[19] Q. Wang, L. Wang, W. Zhu, Q. Xu, Y. Ke, Design optimization of molds for autoclave process of composite manufacturing, J. Reinforc. Plast. Compos. 0 (0) (2007) 13.
[20] N. Kluge, T. Lundstrom, A.L. Ljung, L. Westerberg, T. Nyman, An experimental study of temperature distribution in an autoclave, J. Reinforc. Plast. Compos. 35 (7) (2016) 566–578.
[21] J. Lee, I.Y. Stein, S.S. Kessler, B.L. Wardle, Aligned carbon nanotube film enables thermally induced state transformations in layered polymeric materials, ACS Appl. Mater. Interfaces 7 (16) (2015) 8900–8905.
[22] S.S. Wicks, R.G. de Villoria, B.L. Wardle, Interlaminar and intralaminar reinforcement of composite laminates with aligned carbon nanotubes, Compos. Sci. Technol. 70 (1) (2010) 20–28.
[23] HexPly M56 Product Data Sheet.
[24] Veelo HEAT, General Nano, LLC.
[25] Hexcel, HexPly 8552 Product Data Sheet.
[26] J. Lee, I.Y. Stein, E.F. Antunes, S.S. Kessler, B.L. Wardle, Out-of-oven curing of polymeric composites via resistive microheaters comprised of aligned carbon nanotube networks, in: 20th International Conference on Composite Materials, 2015.
[27] Lindberg/blue M, Linderg/Blue M Gravity Convection Ovens Installation and Operation Manual, 2004.
[28] J. Lee, In situ Curing of Polymeric Composites via Resistive Heaters Comprised of Aligned Carbon Nanotube Networks, Master's thesis, Massachusetts Institute of Technology, 2014.
[29] W. Johnson, P. Mangalgiri, Investigation of fiber bridging in double cantilever beam specimens, J. Compos. Technol. Res. 9 (1) (1987) 10–13.
[30] ASTM-D2344, Standard Test Method for Short-beam Strength of Polymer Matrix Composite Materials and Their Laminates, ASTM International, West Conshohocken PA, 2006.
[31] G. Li, P. Lee-Sullivan, R.W. Thring, Determination of activation energy for glass transition of an epoxy adhesive using dynamic mechanical analysis, J. Therm. Anal. Calorim. 60 (2) (2000) 377–390.
[32] V.M. Karbhari, Q. Wang, Multi-frequency dynamic mechanical thermal analysis of moisture uptake in E-glass/vinylester composites, Compos. B Eng. 35 (4) (2004) 299–304.
[33] L. Barral, J. Cano, A. López, P. Nogueira, C. Ramírez, Determination of the activation energies for α and β transitions of a system containing a diglycidyl ether of bisphenol a (DGEBA) and 1,3-bisaminomethylcyclohexane (1,3-BAC), J. Therm. Anal. 41 (6) (1994) 1463–1467.
[34] W.K. Goertzen, M.R. Kessler, Dynamic mechanical analysis of carbon/epoxy composites for structural pipeline repair, Compos. B Eng. 38 (1) (2007) 1–9.
[35] L. Sperling, Introduction to Physical Polymer Science, John Wiley & Sons, 1992.
[36] A. Rudin, The Elements of Polymer Science and Engineering, Academic press, 1998.
[37] D. Pavlacky, C. Vetter, Thermosetting Polymers vol. 64, CRC Press, 2002.
[38] I.M. Ward, D.W. Hadley, An Introduction to the Mechanical Properties of Solid Polymers, John Wiley & Sons Ltd.; John Wiley & Sons, Inc, 1993.
[39] A.E. Scott, M. Mavrogordato, P. Wright, I. Sinclair, S.M. Spearing, In situ fibre fracture measurement in carbon epoxy laminates using high resolution computed tomography, Compos. Sci. Technol. 71 (12) (2011) 1471–1477.
[40] P. Wright, A. Moffat, I. Sinclair, S.M. Spearing, High resolution tomographic imaging and modelling of notch tip damage in a laminated composite, Compos. Sci. Technol. 70 (10) (2010) 1444–1452.
[41] D. Gürsoy, F. De Carlo, X. Xiao, C. Jacobsen, TomoPy: a framework for the analysis of synchrotron tomographic data, J. Synchrotron Radiat. 21 (5) (2014) 1188–1193.
[42] S.G. Advani, E.M. Sozer, Process Modeling in Composites Manufacturing, vol. 59, CRC Press, 2010.
[43] M. Braun, M. Meyer, 'Pressure Cooker' for Aircraft Components - the World's Largest Research Autoclave Arrives at DLR, DLR German Aerospace Center, 2011.
[44] A. Spaeth, The Black Gold of Stade, Lufthansa magazin.
[45] G. Marsh, Airbus A350 XWB Update, Materials Today, 2010.
[46] B.L. Welch, The generalization of 'Student's' problem when several different population variances are involved, Biometrika 34 (1/2) (1947) 28–35.
[47] K.P. Menard, Dynamic Mechanical Analysis : a Practical Introduction, CRC press, 2008.
[48] B.K. Daniels, N.K. Harakas, R.C. Jackson, Short beam shear tests of graphite fiber composites, Fibre Sci. Technol. 3 (3) (1971) 187–208.
[49] C. Berg, J. Tirosh, M. Israeli, Analysis of short beam bending of fiber reinforced composites, in: Astm Stp, vol. 497, ASTM International, 1972, pp. 206–218.
[50] British standard aerospace series, DIN EN 2563, Carbon Fibre Reinforced Plastics-unidirectional Laminates-determination of the Apparent Interlaminar Shear Strength.
[51] J.W. Tukey, Exploratory Data Analysis, vol. 2, Mass, Reading, 1977.
[52] S. Mortimer, M.J. Smith, E. Olk, Product development for out-of-autoclave (OOA) manufacture of aerospace structure, in: Proceedings of the SAMPE 2010 Conference, 2010. Seattle, WA.
[53] K. Marlett, Y. Ng, J. Tomblin, Hexcel 8552 IM7 unidirectional prepreg 190 gsm & 35% rc qualification material property data report, National Center for Advanced Materials Performance, Wichita, Kansas, 2011, pp. 1–238. Test Report CAM-RP-2009-015, Rev. A.